The RISING Project

Fast Beam Configuration

John Simpson
Hans-Jürgen Wollersheim

CLRC Daresbury Laboratory
Gesellschaft für Schwerionenforschung, Darmstadt

March 2002

1 Introduction

This paper summarises the specification and characteristics of the proposed fast beam set-up for the RISING (**R**are **I**sotope **S**pectroscopic **IN**vestigation at **G**SI) project. The proposed configuration of detectors using a structure that will support up to 15 Cluster Ge detectors and up to 10 Miniball detectors is presented. The layout of the beam line including the proposed beam line tracking and particle detectors is given.

2 Experimental Technique

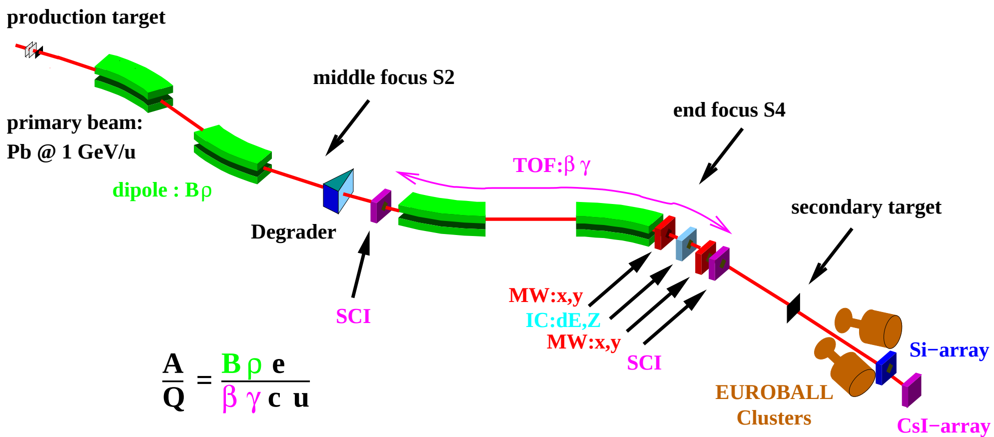

Figure 1: Schematic drawing of the projectile fragment separator FRS with the standard detector set-up for in-flight identification of ions prior to the secondary target.

The proposed γ-ray spectroscopy of radioactive ion beams (RIBs) will be performed after in-flight isotope separation. The nuclei of interest will be produced in fragmentation of stable primary beams or projectile fission of ^{238}U at relativistic energies impinging on a ^{9}Be (target thickness $\approx 1\ g/cm^2\ \equiv 6.7*10^{22}$ target nuclei/cm^2) or ^{208}Pb (target thickness $\approx 1\ g/cm^2\ \equiv 2.9*10^{21}$ target nuclei/cm^2) , which is located at the entrance of the GSI projectile fragment separator FRS. An average beam intensity from the SIS heavy-ion synchrotron between 10^9 medium heavy ions (e.g. ^{129}Xe) and 10^8 ^{208}Pb, ^{238}U per second can be expected. The secondary beam rates can be calculated from the luminosity and the production cross section

$$\textbf{fragments}\ [\mathbf{s^{-1}}] = \textbf{luminosity}\ [\mathbf{cm^{-2}s^{-1}}] * \textbf{cross section}\ [\mathbf{cm^2}]$$

$$\textbf{luminosity}\ [\mathbf{cm^{-2}s^{-1}}] = \textbf{target nuclei}\ [\mathbf{cm^{-2}}] * \textbf{projectiles}\ [\mathbf{s^{-1}}]$$

For fragmentation reactions the online EPAX-program [1] is available, while experimental data are listed for nuclear and electromagnetic fission [2]. **Example:** In case of a ^{129}Xe primary beam impinging on a ^{9}Be target one can expect $4.6*10^{5}$ ^{110}Sn-fragments per second (EPAX cross section: $6.9*10^{-3}$ [b]).

The FRS will be operated in a standard achromatic mode, which allows a separation of fragments by combining magnetic analysis with energy loss in matter. The separated ions will be identified event-by-event with respect to the mass and atomic number (A,Z) via combined time-of-flight, position tracking, and energy loss measurements. The standard detector set-up to identify and track ions from the FRS is shown schematically in figure 1. The **fragment transmission** through the FRS can reach **30% for fragmentation reactions** and is $\approx$ **2% for ^{238}U fission** [3].

3 Experiments with relativistic beams

After passing the identification set-up, the radioactive ions at relativistic energies are focused on a secondary target, which will be positioned approximately 4m after the last FRS-quadrupole in the area S4 [4].

For experiments with beam energies around 100 MeV/u the projectile fragments are analysed after target interaction by a transmission **Si-array (lab. angular range $\pm 3^{0}$)** and a **thick CsI-array (energy resolution $\approx$ 1%)** in order to stop the projectile fragments. A technical drawing of the S4-beamline is available in [5]. The Si-detectors are position sensitive and allow the measurement of the impact parameter for relativistic Coulomb excitation measurements. In these experiments ^{208}Pb targets with a thickness of $0.1-0.4$ g/cm^2 are still acceptable with respect to the angular straggling [6]. The expected excitation cross sections can reach several hundred of millibarns [7], which favours Coulomb excitation for the fast beam campaign.

3.1 The Ge detector array

For the excited fragments moving at a high velocity (v/c=0.43 corresponding to a fragment energy of 100 MeV/u) the γ-detectors have to be positioned at forward and backward angles in order to minimize the Doppler broadening effect. The distance to the target depends on the required energy resolution.

The γ-detectors available to the RISING project are 15 Cluster detectors [8] from the Euroball project [9] and 8 3-way Ge-detectors from the Miniball project [10].

Ring	Detector	Angle	Distance to Target
#1	5 Clusters	$\theta = 15^0$	680mm (fixed)
#2	5 Clusters	$\theta = 26.5^0$	680-1400mm (variable)
#3	5 Clusters	$\theta = 34^0$	680-1400mm (variable)
#4	5 Miniball	$\theta = 46^0$	180-500mm (variable)
#5	5 Miniball	$\theta = 85^0$	180-500mm (variable)

Table 1: Position and distances of the Cluster and Miniball detectors

These detectors will be arranged in rings around the beam pipe (diameter 16cm). As a general rule the detectors will be located at angles and distances (see table 1) to obtain **1% energy resolution for nuclei of velocity v/c=0.43**. Due to the Lorentz boost the main efficiency contribution comes from detectors closest to the beam line in forward direction.

In order to obtain **1% energy resolution** the Clusters have to be located at 680mm, 1119mm and 1369mm in the first, second and third rings, respectively. At these positions the **total efficiency of the Clusters is 1.7%**. The 1^{st} ring of Cluster detectors will be at a fixed distance from the target. For the 2^{nd} and 3^{rd} rings the design will allow the possibility of moving the Cluster detectors closer to the target position, for an increased efficiency but a lower overall energy resolution. If the 2^{nd} and 3^{rd} rings are moved in to 700mm the **total efficiency** will increase to **2.9%** and the overall **energy resolution** reduces to **1.44%**. A schematic layout of the Cluster and Miniball detectors is shown in figure 2.

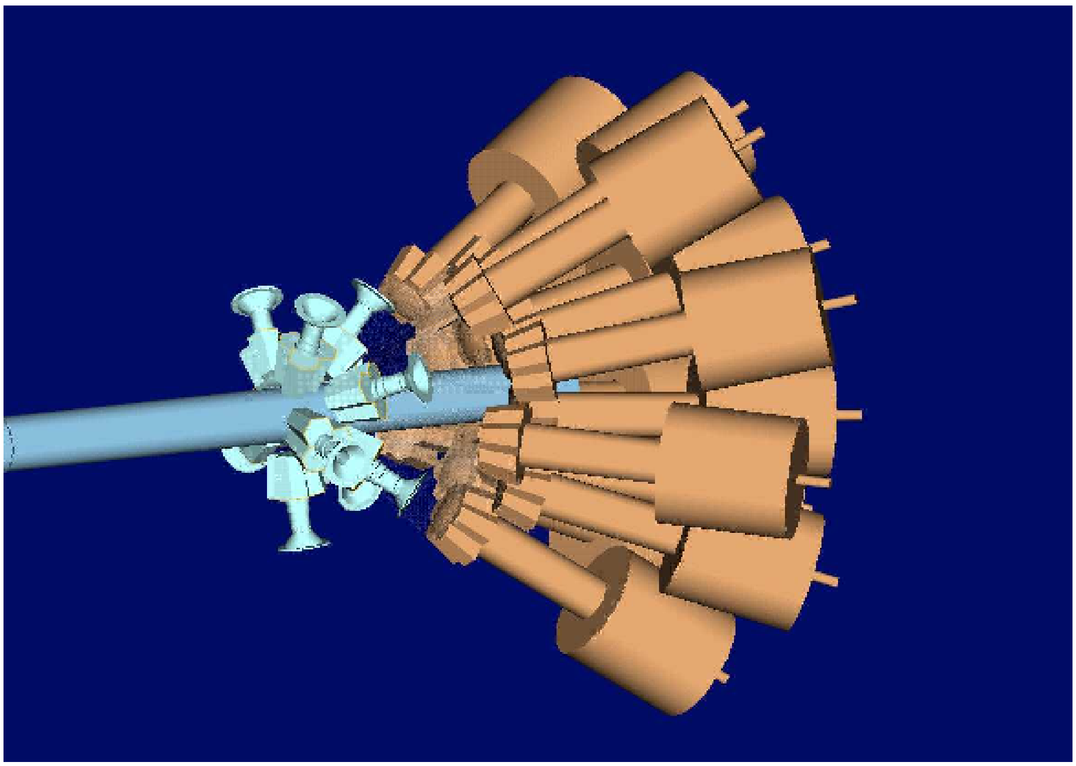

Figure 2: Schematic layout of the Cluster and Miniball detectors in the fast RISING configuration. A 160mm diameter beam pipe passes through the array.

The Miniball detectors can be placed much closer to the target due to their segmentation and the ability to perform pulse shape analysis. The design assumes that the interaction position in the Ge crystal can be determined to 5mm. In the configuration shown in figure 2 there are 5 Miniball detectors at 46^0, 170mm from the target and 3 Miniball detectors at 85^0, 120mm from the target. There is, however, an additional design constraint imposed by the isolated hit probability and the intense atomic background. The scale of this problem depends on the detail of the reaction (beam type, target thickness, etc.) and location of detectors (distance to the target) which must be selected for each experiment.

If a 100 MeV/u ^{238}U beam on a 100 mg/cm^2 ^{208}Pb target is considered, the Miniball detectors can go as close as 400mm to the target before problems become unacceptable. Note that the U beam on a thick Pb target example is a worse case scenario and the minimum distance of 400mm needs to be estimated for each reaction type. At 400mm distance to the target the **8 Miniball detectors** have an **energy resolution** of **0.35**% and a **total efficiency** of **1.2**%.

Adding the 15 Cluster detectors when in the **1**% **energy resolution** position gives a **total efficiency** of **2.9**%. This value increases to **4.2**% if the Clusters are pushed in to 700mm.

For some special experiments with low Z beams and thin targets the Miniball detectors may also be pushed in to 170mm (ring #4, 46^0) and 120mm (ring #5, 85^0), which results in a maximum total efficiency of 9.9% and an average energy resolution of 0.99%.

The Cluster and Miniball detectors will be operated in stand-alone mode without any active suppression shields. Passive suppression will be available to prevent scattering between the Ge crystals in neighbouring detectors.

The array will be supported from below and will split perpendicular to the beam direction by 1m each side to allow access to the target chamber and beam line detectors and for access to the focal plane of the FRS when other experiments are taking place.

3.2 Performance characteristics

The performance of RISING is calculated for a 1.3MeV γ-ray emitted from a fragment moving at v/c=0.43. In these calculations the velocity spread in the target and the ion cone have been ignored. The results are summarised in table 2,3,4. The total energy resolution is a weighted average energy resolution scaled by the efficiency.

Ring	Detector	Angle	Distance mm	Energy Resolution %	Efficiency %
#1	5 Clusters	$\theta = 15^0$	680	0.98	1.06
#2	5 Clusters	$\theta = 26.5^0$	1119	0.99	0.38
#3	5 Clusters	$\theta = 34^0$	1369	0.98	0.25
#1 − 3	15 Clusters			**0.98**	**1.69**
#4	5 Miniball	$\theta = 46^0$	400	0.35	0.87
#5	3 Miniball	$\theta = 85^0$	400	0.37	0.36
#4 − 5	8 Miniball			**0.35**	**1.23**
#1 − 5				**0.72**	**2.93**

Table 2: Performance of an array with Clusters in their 1% energy resolution positions and the Miniball detectors at 400mm.

Ring	Detector	Angle	Distance mm	Energy Resolution %	Efficiency %
#1	5 Clusters	$\theta = 15^0$	680	0.98	1.06
#2	5 Clusters	$\theta = 26.5^0$	700	1.55	0.95
#3	5 Clusters	$\theta = 34^0$	700	1.86	0.90
#1 − 3	15 Clusters			**1.44**	**2.92**
#4	5 Miniball	$\theta = 46^0$	400	0.35	0.87
#5	3 Miniball	$\theta = 85^0$	400	0.37	0.36
#4 − 5	8 Miniball			**0.35**	**1.23**
#1 − 5				**1.11**	**4.15**

Table 3: Performance of an array with Clusters in the 2^{nd} and 3^{rd} rings moved closer to the target (700mm).

Ring	Detector	Angle	Distance mm	Energy Resolution %	Efficiency %
#1	5 Clusters	$\theta = 15^0$	680	0.98	1.06
#2	5 Clusters	$\theta = 26.5^0$	700	1.55	0.95
#3	5 Clusters	$\theta = 34^0$	700	1.86	0.90
#1 − 3	15 Clusters			**1.44**	**2.92**
#4	5 Miniball	$\theta = 46^0$	170	0.70	4.01
#5	3 Miniball	$\theta = 85^0$	120	0.94	2.99
#4 − 5	8 Miniball			**0.80**	**7.00**
#1 − 5				**0.99**	**9.92**

Table 4: Performance of an array with Clusters in the 2^{nd} and 3^{rd} rings moved closer to the target (700mm) and the Miniball detectors moved to 170mm and 120mm in the 4^{th} and 5^{th} rings, respectively. This may be possible in certain experiments where the atomic background is not a severe problem (lower Z beam, thinner target).

References

[1] www-wnt.gsi.de/hellstr/asp/lu-elin/gsi/epaxv21m.asp

[2] www-aix.gsi.de/∼wolle/ISOMER/fission_cross.pdf

[3] www.gsi.de/∼wolle/EB_at_GSI/FRS−WORKING/IMAGES/rates.gif

[4] www.gsi.de/∼wolle/EB_at_GSI/FRS−WORKING/IMAGES/s4_setup.jpg

[5] www.gsi.de/∼wolle/EB_at_GSI/FRS−WORKING/IMAGES/adam.pdf

[6] www.gsi.de/∼wolle/EB_at_GSI/FRS−WORKING/IMAGES/ang_width.gif

[7] www.gsi.de/∼wolle/EB_at_GSI/FRS−WORKING/IMAGES/coulex_cross.gif

[8] J. Eberth et al., Nucl. Instr. Meth. **A369**, 135 (1996)

[9] J. Simpson, Z. Phys. **A358**, 139 (1997)

[10] J. Eberth et al., Proceedings of Erice School 2000 and to be published in Progress in Particle and Nuclear Physics.

4 Appendix-1: www-wnt.gsi.de/hellstr/asp/lu-elin/gsi/epaxv21m.asp

EPAX Version 2.1

An Empirical Parametrization of Projectile-Fragmentation Cross Sections
by K. Sümmerer and B. Blank

Welcome to this interactive version of EPAX V2.1! This program will assist you in estimating production cross sections for projectile fragmentation reaction products, using a parametrization based on experimental data from high-energy reactions.

Please enter the following information:
NOTE: Setting Z(fragment) = 999 calculates *all* possible isotopes (no transfer), while A(fragment)=999 calculates all possible isotopes with Z(fragment)!

Projectile:		*Target:*		*Fragment:*	
A:	58	*A:*	9	*A:*	49
Z:	28	*Z:*	4	*Z:*	28

Calculate the cross section!

If you want to learn more about the EPAX parametrization, such as the underlying physics and the inherent assumptions and limitations, check out these sources:

1. K. Sümmerer *et al.*, Phys. Rev. **C**42, 2546 (1990) [PDF 1457 KB]
2. K. Sümmerer and B. Blank, Phys. Rev. **C**61, 034607 (2000) [PDF 191 KB]
3. K. Sümmerer, "EPAX Version 2: A modified empirical parametrization of fragmentation cross sections"

Remember that in order to obtain production *rates*, the cross sections must be folded with beam intensity and target thickness. Furthermore, the total transmission must be taken into account to predict rates at the final focus of the fragment separator. The program MOCADI can be used for these purposes.

EPAX V2.1 © 1999 K. Sümmerer (GSI-Darmstadt), B. Blank (CEN-Bordeaux)
Active Server Page (ASP) encoding © 2000-2001 M. Hellström (Lund University)

5 Appendix-2: www-aix.gsi.de/~wolle/ISOMER/fission_cross.pdf

Cross sections for isotopic production in U+Be and U+Pb collisions at 750*A MeV from fission and fragmentation

C. Engelmann et al. Z. Phys. A 352 (1995) 351
M. Bernas et al. Phys. Lett. (1997) B415 111

M. Bernas et al. Phys. Lett B331 19 (1994)
C. Donzaud et al. Eur Phys. Jour. A, 1 (1998)
W. Schwab et al. Eur Phys. Jour. A, 2 179 (1998)
J. Benlliure et al. Eur Phys. Jour. A, 2 193 (1998)

Table 5:

$^{238}U + Be$ at 750 AMeV			$^{238}U + Pb$ at 750 AMeV		
fragment	σ (μbarn)	$\Delta\sigma$ (μbarn)	fragment	σ (μbarn)	$\Delta\sigma$ (μbarn)
^{49}Ca	48	5.	^{49}Ca		
^{50}Ca	14	2.	^{50}Ca		
^{51}Ca	2.7	0.2	^{51}Ca		
^{52}Ca	0.45	0.05	^{52}Ca		
^{53}Ca	0.036	0.007	^{53}Ca		
^{54}Ca	0.005	0.001	^{54}Ca		
^{55}Ca	0.002	0.0006	^{55}Ca		
^{56}Ca	0.001	0.0004	^{56}Ca		
^{51}Sc	160.	13.	^{51}Sc		
^{52}Sc	44.	3.	^{52}Sc		
^{53}Sc	14.	1.	^{53}Sc		
^{54}Sc	2.5	0.2	^{54}Sc		
^{55}Sc	0.40	0.04	^{55}Sc		
^{56}Sc	0.05	0.006	^{56}Sc		
^{57}Sc	0.01	0.001	^{57}Sc		
^{58}Sc	0.003	0.0006	^{58}Sc		
^{54}Ti	34.	3.	^{54}Ti		
^{55}Ti	7.4	0.2	^{55}Ti		
^{56}Ti	4.8	0.2	^{56}Ti		
^{57}Ti	0.72	0.04	^{57}Ti		
^{58}Ti	0.19	0.02	^{58}Ti		
^{59}Ti	0.05	0.01	^{59}Ti		
^{60}Ti	0.01	0.002	^{60}Ti		
^{61}Ti	0.0025	0.0008	^{61}Ti		

Table 6:

$^{238}U + Be$ at 750 AMeV			$^{238}U + Pb$ at 750 AMeV		
fragment	σ (μbarn)	$\Delta\sigma$ (μbarn)	fragment	σ (μbarn)	$\Delta\sigma$ (μbarn)
^{56}V	68.	4.	^{56}V		
^{57}V	39.	3.	^{57}V		
^{58}V	9.2	0.4	^{58}V		
^{59}V	4.1	0.2	^{59}V		
^{60}V	0.51	0.04	^{60}V		
^{61}V	0.13	0.01	^{61}V		
^{62}V	0.021	0.003	^{62}V		
^{63}V	0.0064	0.0011	^{63}V		
^{64}V	0.0003	0.0003	^{64}V		
^{59}Cr	55.	4.	^{59}Cr		
^{60}Cr	25.	2.	^{60}Cr		
^{61}Cr	5.2	0.3	^{61}Cr		
^{62}Cr	2.3	0.2	^{62}Cr		
^{63}Cr	0.34	0.03	^{63}Cr		
^{64}Cr	0.072	0.013	^{64}Cr		
^{65}Cr	0.0078	0.0010	^{65}Cr		
^{66}Cr	0.0015	0.0005	^{66}Cr		
^{67}Cr	0.0005	0.0005	^{67}Cr		
^{61}Mn	126.	13.	^{61}Mn		
^{62}Mn	39.	3.	^{62}Mn		
^{63}Mn	24.	2.	^{63}Mn		
^{64}Mn	5.4	0.3	^{64}Mn		
^{65}Mn	1.6	0.1	^{65}Mn		
^{66}Mn	0.22	0.02	^{66}Mn		
^{67}Mn	0.04	0.005	^{67}Mn		
^{68}Mn	0.005	0.0009	^{68}Mn		
^{69}Mn	0.0004	0.0003	^{69}Mn		
^{63}Fe	270.	35.	^{63}Fe		
^{64}Fe	87.	4.	^{64}Fe		
^{65}Fe	37.	2.	^{65}Fe		
^{66}Fe	15.	1.	^{66}Fe		
^{67}Fe	4.9	0.4	^{67}Fe		
^{68}Fe	0.93	0.07	^{68}Fe		
^{69}Fe	0.23	0.03	^{69}Fe		
^{70}Fe	0.028	0.003	^{70}Fe		
^{71}Fe	0.0047	0.0009	^{71}Fe		
^{72}Fe	0.0003	0.0003	^{72}Fe		

Table 7:

$^{238}U + Be$ at 750 AMeV			$^{238}U + Pb$ at 750 AMeV		
fragment	σ (μbarn)	$\Delta\sigma$ (μbarn)	fragment	σ (μbarn)	$\Delta\sigma$ (μbarn)
^{65}Co	194.	45.	^{65}Co		
^{66}Co	150.	8.	^{66}Co		
^{67}Co	72.	4.	^{67}Co		
^{68}Co	24.	2.	^{68}Co		
^{69}Co	12.	0.4	^{69}Co		
^{70}Co	3.1	0.1	^{70}Co		
^{71}Co	0.68	0.04	^{71}Co		
^{72}Co	0.10	0.01	^{72}Co		
^{73}Co	0.02	0.002	^{73}Co		
^{74}Co	0.002	0.0006	^{74}Co		
^{75}Co	0.0003	0.00015	^{75}Co		
^{68}Ni	119.	5.	^{68}Ni		
^{69}Ni	69.	2.	^{69}Ni		
^{70}Ni	35.	1.	^{70}Ni		
^{71}Ni	15.	0.5	^{71}Ni		
^{72}Ni	7.7	0.2	^{72}Ni		
^{73}Ni	2.5	0.1	^{73}Ni		
^{74}Ni	0.63	0.03	^{74}Ni		
^{75}Ni	0.086	0.004	^{75}Ni		
^{76}Ni	0.014	0.001	^{76}Ni		
^{77}Ni	0.0014	0.0004	^{77}Ni		
^{78}Ni	0.0002	0.0001	^{78}Ni		
^{70}Cu	220.	33.	^{70}Cu		
^{71}Cu	143.	17.	^{71}Cu		
^{72}Cu	77.	8.	^{72}Cu		
^{73}Cu	43.	4.	^{73}Cu		
^{74}Cu	20.	2.	^{74}Cu		
^{75}Cu	11.	1.	^{75}Cu		
^{76}Cu	2.7	0.3	^{76}Cu		
^{77}Cu	0.86	0.07	^{77}Cu		
^{78}Cu	0.11	0.01	^{78}Cu		
^{79}Cu	0.015	0.002	^{79}Cu		
^{80}Cu	0.001	0.0005	^{80}Cu		

Table 8:

$^{238}U + Be$ at 750 AMeV			$^{238}U + Pb$ at 750 AMeV		
fragment	σ (μbarn)	$\Delta\sigma$ (μbarn)	fragment	σ (μbarn)	$\Delta\sigma$ (μbarn)
^{73}Zn	227	32.	^{73}Zn		
^{74}Zn	172.	24.	^{74}Zn		
^{75}Zn	94.	10.	^{75}Zn		
^{76}Zn	73.	10.	^{76}Zn		
^{77}Zn	32.	3.	^{77}Zn		
^{78}Zn	16.	2.	^{78}Zn		
^{79}Zn	4.5	0.4	^{79}Zn		
^{80}Zn	1.2	0.1	^{80}Zn		
^{81}Zn	0.13	0.01	^{81}Zn		
^{82}Zn	0.013	0.002	^{82}Zn		
^{83}Zn	0.001	0.0004	^{83}Zn		
^{76}Ga	242.	7.	^{76}Ga		
^{77}Ga	193.	4.	^{77}Ga		
^{78}Ga	144.	3.	^{78}Ga	790.	190.
^{79}Ga	106.	1.	^{79}Ga	550.	130.
^{80}Ga	51.	1.	^{80}Ga	320.	70.
^{81}Ga	22.	0.4	^{81}Ga	120.	10.
^{82}Ga	4.3	0.1	^{82}Ga	33.	9.
^{83}Ga	0.81	0.02	^{83}Ga		
^{84}Ga	0.10	0.005	^{84}Ga		
^{85}Ga	0.0065	0.0009	^{85}Ga		
^{86}Ga	0.0006	0.0003	^{86}Ga		
^{72}Ge			^{72}Ge	7300.	4000.
^{73}Ge			^{73}Ge		
^{74}Ge			^{74}Ge	10000.	1000.
^{75}Ge			^{75}Ge	8500.	800.
^{76}Ge			^{76}Ge	7500.	800.
^{77}Ge			^{77}Ge	4300.	500.
^{78}Ge	370.	7.	^{78}Ge	1700.	300.
^{79}Ge	371.	7.	^{79}Ge	3300.	900.
^{80}Ge	323.	6.	^{80}Ge	4600.	1000.
^{81}Ge	291.	3.	^{81}Ge	4600.	600.
^{82}Ge	207.	2.	^{82}Ge	4240.	600.
^{83}Ge	76.	1.	^{83}Ge	1700.	150.
^{84}Ge	29.	0.3	^{84}Ge	500.	40.
^{85}Ge	4.7	0.1	^{85}Ge	130.	30.
^{86}Ge	0.82	0.02	^{86}Ge	70.	30.
^{87}Ge	0.067	0.003	^{87}Ge		
^{88}Ge	0.0067	0.0009	^{88}Ge		
^{89}Ge	0.0006	0.0003	^{89}Ge		

Table 9:

$^{238}U + Be$ at 750 AMeV			$^{238}U + Pb$ at 750 AMeV		
fragment	σ (μbarn)	$\Delta\sigma$ (μbarn)	fragment	σ (μbarn)	$\Delta\sigma$ (μbarn)
^{75}As			^{75}As	6700.	4000.
^{76}As			^{76}As	10900.	1000.
^{77}As			^{77}As	12200.	1100.
^{78}As			^{78}As	8700.	800.
^{79}As			^{79}As	5800.	600.
^{80}As			^{80}As	4200.	600.
^{81}As			^{81}As	7400.	2400.
^{82}As	535.	11.	^{82}As	7200.	1400.
^{83}As	503.	10.	^{83}As	10600.	1300.
^{84}As	394.	4.	^{84}As	6600.	600.
^{85}As	247.	2.	^{85}As	5300.	700.
^{86}As	73.	0.7	^{86}As	1700.	100.
^{87}As	19.	0.4	^{87}As	520.	50.
^{88}As	2.9	0.09	^{88}As	73.	20.
^{89}As	0.34	0.01	^{89}As	7.	2.
^{90}As	0.021	0.002	^{90}As		
^{91}As	0.0032	0.0008	^{91}As		
^{92}As	0.0006	0.0003	^{92}As		
^{77}Se			^{77}Se	6550.	3000.
^{78}Se			^{78}Se	14700.	1300.
^{79}Se			^{79}Se	14900.	1200.
^{80}Se			^{80}Se	15200.	1300.
^{81}Se			^{81}Se	9600.	600.
^{82}Se			^{82}Se	6760.	1000.
^{83}Se	1360.	27.	^{83}Se	9120.	3100.
^{84}Se	1150.	12.	^{84}Se	18610.	3000.
^{85}Se	870.	261.	^{85}Se	20620.	2700.
^{86}Se	910.	9.	^{86}Se	22200.	1300.
^{87}Se	536.	5.	^{87}Se	14230.	1700.
^{88}Se	279.	3.	^{88}Se	7130.	1000.
^{89}Se	61.	0.6	^{89}Se	1630.	80.
^{90}Se	14.	0.3	^{90}Se	400.	50.
^{91}Se	1.1	0.02	^{91}Se	31.	15.
^{92}Se	0.12	0.005	^{92}Se		
^{93}Se	0.008	0.001	^{93}Se		
^{94}Se	0.002	0.0005	^{94}Se		

Table 10:

$^{238}U + Be$ at 750 AMeV			$^{238}U + Pb$ at 750 AMeV		
fragment	σ (μbarn)	$\Delta\sigma$ (μbarn)	fragment	σ (μbarn)	$\Delta\sigma$ (μbarn)
^{79}Br			^{79}Br	7900.	3000.
^{80}Br			^{80}Br		
^{81}Br			^{81}Br	17350.	1300.
^{82}Br			^{82}Br	17400.	1400.
^{83}Br			^{83}Br	14600.	1200.
^{84}Br			^{84}Br	11200.	1000.
^{85}Br			^{85}Br	10900.	3000.
^{86}Br	1360.	14.	^{86}Br	21250.	6200.
^{87}Br	1280.	13.	^{87}Br	30560.	3000.
^{88}Br	960.	480.	^{88}Br	37440.	4800.
^{89}Br	1020.	10.	^{89}Br	25900.	1300.
^{90}Br	447.	4.	^{90}Br	14900.	2500.
^{91}Br	238.	2.	^{91}Br	5940.	500.
^{92}Br	34.	0.3	^{92}Br	890.	50.
^{93}Br	8.2	0.16	^{93}Br	230.	40.
^{94}Br	0.67	0.02	^{94}Br		
^{95}Br	0.075	0.003	^{95}Br		
^{96}Br	0.0059	0.0008	^{96}Br		
^{97}Br	0.0007	0.0003	^{97}Br		
^{79}Kr			^{79}Kr	3750.	2000.
^{80}Kr			^{80}Kr	8370.	4800.
^{81}Kr			^{81}Kr	10900.	4500.
^{82}Kr			^{82}Kr		
^{83}Kr			^{83}Kr	16000.	1400.
^{84}Kr			^{84}Kr	19100.	1600.
^{85}Kr			^{85}Kr	17100.	1400.
^{86}Kr			^{86}Kr	13300.	1800.
^{87}Kr			^{87}Kr	10000.	2600.
^{88}Kr			^{88}Kr	26400.	8400.
^{89}Kr	2170.	22.	^{89}Kr	49600.	6000.
^{90}Kr	1600.	16.	^{90}Kr	59400.	5000.
^{91}Kr	1580.	16.	^{91}Kr	58600.	3800.
^{92}Kr	1290.	13.	^{92}Kr	32600.	1400.
^{93}Kr	467.	5.	^{93}Kr	15300.	1700.
^{94}Kr	168.	1.7	^{94}Kr	4840.	240.
^{95}Kr	29.	0.3	^{95}Kr	800.	50.
^{96}Kr	6.	0.1	^{96}Kr	180.	30.
^{97}Kr	0.5	0.015	^{97}Kr		
^{98}Kr	0.054	0.003	^{98}Kr		
^{99}Kr	0.0026	0.0005	^{99}Kr		
^{100}Kr	0.0005	0.0003	^{100}Kr		

Table 11:

$^{238}U + Be$ at 750 AMeV			$^{238}U + Pb$ at 750 AMeV		
fragment	σ (μbarn)	$\Delta\sigma$ (μbarn)	fragment	σ (μbarn)	$\Delta\sigma$ (μbarn)
^{82}Rb			^{82}Rb	2800.	1100.
^{83}Rb			^{83}Rb	10300.	5000.
^{84}Rb			^{84}Rb	9500.	4000.
^{85}Rb			^{85}Rb	18100.	2400.
^{86}Rb			^{86}Rb	18700.	1500.
^{87}Rb			^{87}Rb	21400.	1700.
^{88}Rb			^{88}Rb	16400.	1400.
^{89}Rb			^{89}Rb	13700.	3600.
^{90}Rb			^{90}Rb	18900.	5400.
^{91}Rb	3000.	30.	^{91}Rb	49500.	10900.
^{92}Rb	2040.	204.	^{92}Rb	57800.	4200.
^{93}Rb	1300.	650.	^{93}Rb	65440.	7200.
^{94}Rb	1450.	15.	^{94}Rb	42800.	1750.
^{95}Rb	1040.	10.	^{95}Rb	29340.	3800.
^{96}Rb	323.	3.	^{96}Rb	10440.	870.
^{97}Rb	122.	1.	^{97}Rb	3090.	110.
^{98}Rb	18.	0.4	^{98}Rb	490.	50.
^{99}Rb	3.2	0.1	^{99}Rb	95.	20.
^{100}Rb	0.23	0.01	^{100}Rb		
^{101}Rb	0.025	0.002	^{101}Rb		
^{102}Rb	0.0009	0.0003	^{102}Rb		

Table 12:

$^{238}U+Be$ at 750 AMeV			$^{238}U+Pb$ at 750 AMeV		
fragment	σ (μbarn)	$\Delta\sigma$ (μbarn)	fragment	σ (μbarn)	$\Delta\sigma$ (μbarn)
^{84}Sr			^{84}Sr	320.	170.
^{85}Sr			^{85}Sr	1570.	900.
^{86}Sr			^{86}Sr	5250.	2410.
^{87}Sr			^{87}Sr	8000.	3000.
^{88}Sr			^{88}Sr	18000.	1400.
^{89}Sr			^{89}Sr	20000.	2500.
^{90}Sr			^{90}Sr	19700.	2500.
^{91}Sr			^{91}Sr	13400.	5000.
^{92}Sr			^{92}Sr	20560.	7200.
^{93}Sr			^{93}Sr	37300.	12000.
^{94}Sr	2540.	25.	^{94}Sr	58700.	8800.
^{95}Sr	1950.	20.	^{95}Sr	72000.	4600.
^{96}Sr	1180.	590.	^{96}Sr	78600.	6700.
^{97}Sr	1460.	15.	^{97}Sr	42700.	1500.
^{98}Sr	856.	9.	^{98}Sr	30700.	3700.
^{99}Sr	223.	2.	^{99}Sr	7100.	550.
^{100}Sr	53.	0.5	^{100}Sr	1790.	70.
^{101}Sr	7.9	0.2	^{101}Sr	260.	30.
^{102}Sr	0.94	0.03	^{102}Sr		
^{103}Sr	0.05	0.003	^{103}Sr		
^{104}Sr	0.0066	0.0009	^{104}Sr		
^{105}Sr	0.0008	0.0005	^{105}Sr		

Table 13:

$^{238}U + Be$ at 750 AMeV			$^{238}U + Pb$ at 750 AMeV		
fragment	σ (μbarn)	$\Delta\sigma$ (μbarn)	fragment	σ (μbarn)	$\Delta\sigma$ (μbarn)
^{86}Y			^{86}Y	2000.	1100.
^{87}Y			^{87}Y	9200.	4230.
^{88}Y			^{88}Y	11400.	4700.
^{89}Y			^{89}Y		
^{90}Y			^{90}Y	18340.	1500.
^{91}Y			^{91}Y	20100.	1600.
^{92}Y			^{92}Y	22600.	2900.
^{93}Y			^{93}Y	17700.	1500.
^{94}Y			^{94}Y	16500.	4000.
^{95}Y			^{95}Y	25150.	5800.
^{96}Y			^{96}Y	43400.	7300.
^{97}Y			^{97}Y	66000.	5000.
^{98}Y			^{98}Y	62300.	5000.
^{99}Y	1580.	16.	^{99}Y	68100.	3400.
^{100}Y	1250.	13.	^{100}Y	28000.	1100.
^{101}Y	514.	5.	^{101}Y	14800.	1600.
^{102}Y	124.	1.	^{102}Y	3110.	180.
^{103}Y	24.	0.2	^{103}Y	590.	40.
^{104}Y	2.8	0.1	^{104}Y	70.	10.
^{105}Y	0.31	0.02	^{105}Y	10.	3.
^{106}Y	0.016	0.002	^{106}Y		
^{107}Y	0.0028	0.0007	^{107}Y		

Table 14:

$^{238}U + Be$ at 750 AMeV			$^{238}U + Pb$ at 750 AMeV		
fragment	σ (μbarn)	$\Delta\sigma$ (μbarn)	fragment	σ (μbarn)	$\Delta\sigma$ (μbarn)
^{88}Zr			^{88}Zr	2000.	1800.
^{89}Zr			^{89}Zr	8800.	5000.
^{90}Zr			^{90}Zr	12000.	5000.
^{91}Zr			^{91}Zr	10000.	3000.
^{92}Zr			^{92}Zr	16400.	2100.
^{93}Zr			^{93}Zr	18400.	1400.
^{94}Zr			^{94}Zr	24100.	3100.
^{95}Zr			^{95}Zr	21500.	2700.
^{96}Zr			^{96}Zr	19300.	2500.
^{97}Zr			^{97}Zr	21400.	7500.
^{98}Zr			^{98}Zr	37100.	12200.
^{99}Zr	2560.	26.	^{99}Zr	70000.	10000.
^{100}Zr	2410.	24.	^{100}Zr	86300.	4500.
^{101}Zr	1240.	620.	^{101}Zr	73100.	5000.
^{102}Zr	1390.	14.	^{102}Zr	52600.	1700.
^{103}Zr	674.	7.	^{103}Zr	22000.	1900.
^{104}Zr	280.	3.	^{104}Zr	8700.	700.
^{105}Zr	50.	0.5	^{105}Zr	1150.	70.
^{106}Zr	9.1	0.2	^{106}Zr	210.	20.
^{107}Zr	0.88	0.04	^{107}Zr	25.	10.
^{108}Zr	0.10	0.006	^{108}Zr		
^{109}Zr	0.0054	0.0008	^{109}Zr		
^{110}Zr	0.0004	0.0002	^{110}Zr		

Table 15:

$^{238}U + Be$ at 750 AMeV			$^{238}U + Pb$ at 750 AMeV		
fragment	σ (μbarn)	$\Delta\sigma$ (μbarn)	fragment	σ (μbarn)	$\Delta\sigma$ (μbarn)
^{90}Nb			^{90}Nb	3360.	1800.
^{91}Nb			^{91}Nb	6870.	4200.
^{92}Nb			^{92}Nb	11250.	5100.
^{93}Nb			^{93}Nb	10120.	4200.
^{94}Nb			^{94}Nb	13900.	4200.
^{95}Nb			^{95}Nb	17200.	1300.
^{96}Nb			^{96}Nb	20400.	2600.
^{97}Nb			^{97}Nb	24000.	3000.
^{98}Nb			^{98}Nb	18300.	1500.
^{99}Nb			^{99}Nb	17300.	2200.
^{100}Nb			^{100}Nb	22000.	7500.
^{101}Nb			^{101}Nb	39800.	12700.
^{102}Nb			^{102}Nb	55300.	6600.
^{103}Nb			^{103}Nb	56900.	3900.
^{104}Nb			^{104}Nb	38900.	4300.
^{105}Nb	1800.	180.	^{105}Nb	19200.	900.
^{106}Nb	383.	4.	^{106}Nb	6340.	950.
^{107}Nb	134.	1.	^{107}Nb	1850.	220.
^{108}Nb	25.	1.	^{108}Nb	240.	29.
^{109}Nb	4.5	0.1	^{109}Nb	41.	13.
^{110}Nb	0.48	0.03	^{110}Nb	6.	3.
^{111}Nb	0.05	0.005	^{111}Nb		
^{112}Nb	0.0025	0.0006	^{112}Nb		
^{113}Nb	0.0007	0.0003	^{113}Nb		

Table 16:

$^{238}U + Be$ at 750 AMeV			$^{238}U + Pb$ at 750 AMeV		
fragment	σ (μbarn)	$\Delta\sigma$ (μbarn)	fragment	σ (μbarn)	$\Delta\sigma$ (μbarn)
^{92}Mo			^{92}Mo	2070.	1300.
^{93}Mo			^{93}Mo	4770.	2300.
^{94}Mo			^{94}Mo	8450.	3600.
^{95}Mo			^{95}Mo	12010.	3700.
^{96}Mo			^{96}Mo	15000.	4000.
^{97}Mo			^{97}Mo	16500.	2100.
^{98}Mo			^{98}Mo	19400.	2500.
^{99}Mo			^{99}Mo	26500.	6900.
^{100}Mo			^{100}Mo	23300.	6100.
^{101}Mo			^{101}Mo	19400.	2500.
^{102}Mo			^{102}Mo	15500.	5000.
^{103}Mo			^{103}Mo	30000.	7000.
^{104}Mo			^{104}Mo	44300.	10000.
^{105}Mo			^{105}Mo	41500.	4100.
^{106}Mo			^{106}Mo	30500.	3000.
^{107}Mo			^{107}Mo	16200.	1500.
^{108}Mo			^{108}Mo	7000.	500.
^{109}Mo			^{109}Mo	1970.	280.
^{110}Mo			^{110}Mo	550.	70.
^{111}Mo			^{111}Mo	71.	14.
^{112}Mo			^{112}Mo	12.	5.
^{113}Mo			^{113}Mo		
^{114}Mo	0.024	0.009	^{114}Mo		

Table 17:

$^{238}U + Be$ at 750 AMeV			$^{238}U + Pb$ at 750 AMeV		
fragment	σ (μbarn)	$\Delta\sigma$ (μbarn)	fragment	σ (μbarn)	$\Delta\sigma$ (μbarn)
^{94}Tc			^{94}Tc	1707.	800.
^{95}Tc			^{95}Tc	3720.	1500.
^{96}Tc			^{96}Tc	5900.	2700.
^{97}Tc			^{97}Tc	8020.	3320.
^{98}Tc			^{98}Tc		
^{99}Tc			^{99}Tc	14190.	2000.
^{100}Tc			^{100}Tc	15800.	1200.
^{101}Tc			^{101}Tc	20200.	2500.
^{102}Tc			^{102}Tc	23500.	3000.
^{103}Tc			^{103}Tc	23700.	1800.
^{104}Tc			^{104}Tc	18700.	1400.
^{105}Tc			^{105}Tc	19900.	6000.
^{106}Tc			^{106}Tc	18200.	5500.
^{107}Tc			^{107}Tc	24200.	6500.
^{108}Tc			^{108}Tc	19800.	2400.
^{109}Tc			^{109}Tc	14200.	1700.
^{110}Tc			^{110}Tc	7800.	900.
^{111}Tc			^{111}Tc	2910.	700.
^{112}Tc			^{112}Tc	850.	200.
^{113}Tc			^{113}Tc	220.	40.
^{114}Tc			^{114}Tc	25.	7.
^{115}Tc			^{115}Tc	9.	4.
^{116}Tc	0.081	0.016	^{116}Tc		
^{117}Tc	0.0084	0.0050	^{117}Tc		

Table 18:

$^{238}U + Be$ at 750 AMeV			$^{238}U + Pb$ at 750 AMeV		
fragment	σ (μbarn)	$\Delta\sigma$ (μbarn)	fragment	σ (μbarn)	$\Delta\sigma$ (μbarn)
^{98}Ru			^{98}Ru	5550.	2550.
^{99}Ru			^{99}Ru	7000.	3200.
^{100}Ru			^{100}Ru	7530.	3140.
^{101}Ru			^{101}Ru	12800.	2600.
^{102}Ru			^{102}Ru	14900.	1100.
^{103}Ru			^{103}Ru	18100.	1400.
^{104}Ru			^{104}Ru	23400.	6100.
^{105}Ru			^{105}Ru	21100.	2700.
^{106}Ru			^{106}Ru	19300.	2400.
^{107}Ru			^{107}Ru	16900.	4500.
^{108}Ru			^{108}Ru	14500.	6000.
^{109}Ru			^{109}Ru	19300.	6400.
^{110}Ru			^{110}Ru	21500.	4300.
^{111}Ru			^{111}Ru	14500.	1600.
^{112}Ru			^{112}Ru	10100.	1400.
^{113}Ru			^{113}Ru	4370.	500.
^{114}Ru			^{114}Ru	1570.	200.
^{115}Ru			^{115}Ru	480.	100.
^{116}Ru			^{116}Ru	110.	20.
^{117}Ru			^{117}Ru	20.	8.
^{118}Ru			^{118}Ru		
^{119}Ru	0.014	0.006	^{119}Ru		

Table 19:

$^{238}U + Be$ at 750 AMeV			$^{238}U + Pb$ at 750 AMeV		
fragment	σ (μbarn)	$\Delta\sigma$ (μbarn)	fragment	σ (μbarn)	$\Delta\sigma$ (μbarn)
^{99}Rh			^{99}Rh	1220.	670.
^{100}Rh			^{100}Rh	5360.	2460.
^{101}Rh			^{101}Rh	6000.	2800.
^{102}Rh			^{102}Rh	6500.	2000.
^{103}Rh			^{103}Rh		
^{104}Rh			^{104}Rh	12500.	1000.
^{105}Rh			^{105}Rh	14600.	1100.
^{106}Rh			^{106}Rh	17700.	2200.
^{107}Rh			^{107}Rh	20500.	5300.
^{108}Rh			^{108}Rh	18200.	1400.
^{109}Rh			^{109}Rh	16400.	1300.
^{110}Rh			^{110}Rh	14300.	3800.
^{111}Rh			^{111}Rh	16500.	4610.
^{112}Rh			^{112}Rh	17300.	4700.
^{113}Rh			^{113}Rh	18030.	2300.
^{114}Rh			^{114}Rh	10400.	1100.
^{115}Rh			^{115}Rh	7000.	1050.
^{116}Rh			^{116}Rh	2740.	300.
^{117}Rh			^{117}Rh	1000.	200.
^{118}Rh			^{118}Rh	230.	70.
^{119}Rh			^{119}Rh	45.	20.
^{120}Rh			^{120}Rh	4.	2.
^{121}Rh			^{121}Rh		
^{122}Rh	0.013	0.006	^{122}Rh		

Table 20:

$^{238}U + Be$ at 750 AMeV			$^{238}U + Pb$ at 750 AMeV		
fragment	σ (μbarn)	$\Delta\sigma$ (μbarn)	fragment	σ (μbarn)	$\Delta\sigma$ (μbarn)
^{101}Pd			^{101}Pd	780.	450.
^{102}Pd			^{102}Pd	2960.	1840.
^{103}Pd			^{103}Pd	5320.	2210.
^{104}Pd			^{104}Pd	4700.	2000.
^{105}Pd			^{105}Pd	9100.	1400.
^{106}Pd			^{106}Pd	12600.	1600.
^{107}Pd			^{107}Pd	13700.	1100.
^{108}Pd			^{108}Pd	16700.	1300.
^{109}Pd			^{109}Pd	21900.	5700.
^{110}Pd			^{110}Pd	19700.	2500.
^{111}Pd			^{111}Pd	16200.	1200.
^{112}Pd			^{112}Pd	14600.	1100.
^{113}Pd			^{113}Pd	13500.	3800.
^{114}Pd			^{114}Pd	15300.	3100.
^{115}Pd			^{115}Pd	18100.	3000.
^{116}Pd			^{116}Pd	14600.	1700.
^{117}Pd			^{117}Pd	9250.	1200.
^{118}Pd			^{118}Pd	5020.	650.
^{119}Pd			^{119}Pd	1900.	270.
^{120}Pd			^{120}Pd	640.	140.
^{121}Pd			^{121}Pd	160.	40.
^{122}Pd			^{122}Pd	40.	10.
^{123}Pd			^{123}Pd	10.	4.

Table 21:

$^{238}U + Be$ at 750 AMeV			$^{238}U + Pb$ at 750 AMeV		
fragment	σ (μbarn)	$\Delta\sigma$ (μbarn)	fragment	σ (μbarn)	$\Delta\sigma$ (μbarn)
^{103}Ag			^{103}Ag	300.	130.
^{104}Ag			^{104}Ag	1000.	640.
^{105}Ag			^{105}Ag	3850.	1600.
^{106}Ag			^{106}Ag	3820.	1600.
^{107}Ag			^{107}Ag		
^{108}Ag			^{108}Ag	9000.	1000.
^{109}Ag			^{109}Ag	11700.	1000.
^{110}Ag			^{110}Ag	14600.	1100.
^{111}Ag			^{111}Ag	17900.	2300.
^{112}Ag			^{112}Ag	20800.	5400.
^{113}Ag			^{113}Ag	18000.	1400.
^{114}Ag			^{114}Ag	15600.	1200.
^{115}Ag			^{115}Ag	13900.	1800.
^{116}Ag			^{116}Ag	14200.	3400.
^{117}Ag			^{117}Ag	15440.	3500.
^{118}Ag			^{118}Ag	15700.	2300.
^{119}Ag			^{119}Ag	11300.	1500.
^{120}Ag			^{120}Ag	6500.	1000.
^{121}Ag			^{121}Ag	3700.	500.
^{122}Ag			^{122}Ag	1250.	200.
^{123}Ag			^{123}Ag	570.	160.
^{124}Ag			^{124}Ag	150.	40.
^{125}Ag			^{125}Ag	47.	11.
^{126}Ag			^{126}Ag	8.	3.

Table 22:

$^{238}U + Be$ at 750 AMeV			$^{238}U + Pb$ at 750 AMeV		
fragment	σ (μbarn)	$\Delta\sigma$ (μbarn)	fragment	σ (μbarn)	$\Delta\sigma$ (μbarn)
^{107}Cd			^{107}Cd	460.	340.
^{108}Cd			^{108}Cd	1510.	690.
^{109}Cd			^{109}Cd	1740.	750.
^{110}Cd			^{110}Cd		
^{111}Cd			^{111}Cd	8800.	1100.
^{112}Cd			^{112}Cd	11600.	1500.
^{113}Cd			^{113}Cd	14700.	1100.
^{114}Cd			^{114}Cd	18700.	2400.
^{115}Cd			^{115}Cd	18200.	2400.
^{116}Cd			^{116}Cd	14900.	1200.
^{117}Cd			^{117}Cd	14200.	1800.
^{118}Cd			^{118}Cd	13500.	3500.
^{119}Cd			^{119}Cd	11700.	3100.
^{120}Cd			^{120}Cd	14400.	3300.
^{121}Cd			^{121}Cd	11100.	2200.
^{122}Cd			^{122}Cd	9500.	1000.
^{123}Cd			^{123}Cd	6000.	800.
^{124}Cd			^{124}Cd	3500.	350.
^{125}Cd			^{125}Cd	2030.	260.
^{126}Cd			^{126}Cd	1240.	220.
^{127}Cd			^{127}Cd		
^{128}Cd			^{128}Cd	160.	20.
^{129}Cd			^{129}Cd	25.	6.

Table 23:

$^{238}U + Be$ at 750 AMeV			$^{238}U + Pb$ at 750 AMeV		
fragment	σ (μbarn)	$\Delta\sigma$ (μbarn)	fragment	σ (μbarn)	$\Delta\sigma$ (μbarn)
^{108}In			^{108}In	1250.	900.
^{109}In			^{109}In	2360.	1080.
^{110}In			^{110}In	3050.	1270.
^{111}In			^{111}In		
^{112}In			^{112}In		
^{113}In			^{113}In		
^{114}In			^{114}In	10200.	800.
^{115}In			^{115}In	12000.	1000.
^{116}In			^{116}In	14600.	1900.
^{117}In			^{117}In	16500.	2100.
^{118}In			^{118}In	16100.	1200.
^{119}In			^{119}In	13500.	1100.
^{120}In			^{120}In	13100.	1700.
^{121}In			^{121}In	13400.	2600.
^{122}In			^{122}In	14600.	3100.
^{123}In			^{123}In	14900.	3000.
^{124}In			^{124}In	10500.	1200.
^{125}In			^{125}In	8900.	1000.
^{126}In			^{126}In	6900.	800.
^{127}In			^{127}In	5030.	450.
^{128}In			^{128}In	4200.	600.
^{129}In			^{129}In	3100.	500.
^{130}In			^{130}In	1150.	110.
^{131}In			^{131}In	290.	20.
^{132}In			^{132}In	32.	7.

Table 24:

$^{238}U + Be$ at 750 AMeV			$^{238}U + Pb$ at 750 AMeV		
fragment	σ (μbarn)	$\Delta\sigma$ (μbarn)	fragment	σ (μbarn)	$\Delta\sigma$ (μbarn)
^{111}Sn			^{111}Sn	1900.	900.
^{112}Sn			^{112}Sn	2300.	900.
^{113}Sn			^{113}Sn		
^{114}Sn			^{114}Sn		
^{115}Sn			^{115}Sn		
^{116}Sn			^{116}Sn	5600.	700.
^{117}Sn			^{117}Sn	8100.	1100.
^{118}Sn			^{118}Sn	10600.	900.
^{119}Sn			^{119}Sn	11000.	2900.
^{120}Sn			^{120}Sn	13800.	1700.
^{121}Sn			^{121}Sn	12300.	900.
^{122}Sn			^{122}Sn	10500.	2400.
^{123}Sn			^{123}Sn	9300.	2300.
^{124}Sn			^{124}Sn	11200.	3200.
^{125}Sn			^{125}Sn	11100.	3900.
^{126}Sn			^{126}Sn	13000.	3100.
^{127}Sn			^{127}Sn	13900.	1400.
^{128}Sn			^{128}Sn	16400.	1500.
^{129}Sn			^{129}Sn	20600.	1200.
^{130}Sn			^{130}Sn	25700.	900.
^{131}Sn			^{131}Sn	23200.	1900.
^{132}Sn			^{132}Sn	15400.	1400.
^{133}Sn			^{133}Sn	2590.	110.
^{134}Sn			^{134}Sn	476.	26.
^{135}Sn			^{135}Sn	67.	11.
^{136}Sn			^{136}Sn	13.	5.

Table 25:

$^{238}U + Be$ at 750 AMeV			$^{238}U + Pb$ at 750 AMeV		
fragment	σ (μbarn)	$\Delta\sigma$ (μbarn)	fragment	σ (μbarn)	$\Delta\sigma$ (μbarn)
^{114}Sb			^{114}Sb	1700.	800.
^{115}Sb			^{115}Sb		
^{116}Sb			^{116}Sb		
^{117}Sb			^{117}Sb		
^{118}Sb			^{118}Sb		
^{119}Sb			^{119}Sb		
^{120}Sb			^{120}Sb		
^{121}Sb			^{121}Sb	9700.	2500.
^{122}Sb			^{122}Sb	11600.	1500.
^{123}Sb			^{123}Sb	12300.	1000.
^{124}Sb			^{124}Sb	11200.	900.
^{125}Sb			^{125}Sb	9300.	1200.
^{126}Sb			^{126}Sb	8300.	2700.
^{127}Sb			^{127}Sb	13000.	3680.
^{128}Sb			^{128}Sb	14100.	4100.
^{129}Sb			^{129}Sb	16400.	2500.
^{130}Sb			^{130}Sb	24100.	1800.
^{131}Sb			^{131}Sb	41200.	3000.
^{132}Sb			^{132}Sb	47500.	1900.
^{133}Sb			^{133}Sb	45000.	1400.
^{134}Sb			^{134}Sb	16800.	1600.
^{135}Sb			^{135}Sb	5900.	470.
^{136}Sb			^{136}Sb	1100.	60.
^{137}Sb			^{137}Sb	180.	20.
^{138}Sb			^{138}Sb	23.	6.
^{139}Sb			^{139}Sb	5.	2.

6 Appendix-3:

www.gsi.de/∼wolle/EB_at_GSI/FRS-WORKING/IMAGES/rates.gif

Secondary beam rates

Ion (S4 energy)	Reaction	σ_{prod} [barn]	N_{Target}	ε_{FRS}	R(S4) [per proj.]
^{48}Cr 100 MeV/u	$^{58}Ni + Be$ proj.frag.	$2.4 * 10^{-3}$	$2.9 * 10^{23}$ ($4.3\ g/cm^2$)	0.22	$1.6 * 10^{-4}$
^{56}Ni 100 MeV/u	$^{58}Ni + Be$ proj.frag.	$2.7 * 10^{-3}$	$4.0 * 10^{23}$ ($6.0\ g/cm^2$)	0.33	$3.6 * 10^{-4}$
^{190}W 100 MeV/u	$^{238}U + Be$ proj.frag.	$3.7 * 10^{-7}$	$1.0 * 10^{23}$ ($1.5\ g/cm^2$)	0.045	$1.7 * 10^{-9}$
^{132}Sn 100 MeV/u	$^{238}U + Be$ fission	$3.0 * 10^{-4}$	$2.0 * 10^{23}$ ($3.0\ g/cm^2$)	0.019	$1.1 * 10^{-6}$
^{132}Sn 100 MeV/u	$^{238}U + Pb$ fission	$(1.5 \pm .1) * 10^{-2}$	$3.8 * 10^{21}$ ($1.3\ g/cm^2$)	0.019	$1.1 * 10^{-6}$
^{56}Ni 10 MeV/u	$^{58}Ni + Be$ proj.frag.	$2.7 * 10^{-3}$	$4.0 * 10^{23}$ ($6.0\ g/cm^2$)	0.17	$1.6 * 10^{-4}$
^{190}W 10 MeV/u	$^{238}U + Be$ proj.frag.	$3.7 * 10^{-7}$	$1.0 * 10^{23}$ ($1.5\ g/cm^2$)	0.035	$1.3 * 10^{-9}$

7 Appendix-4:

www.gsi.de/∼wolle/EB_at_GSI/FRS-WORKING/IMAGES/s4_setup.jpg

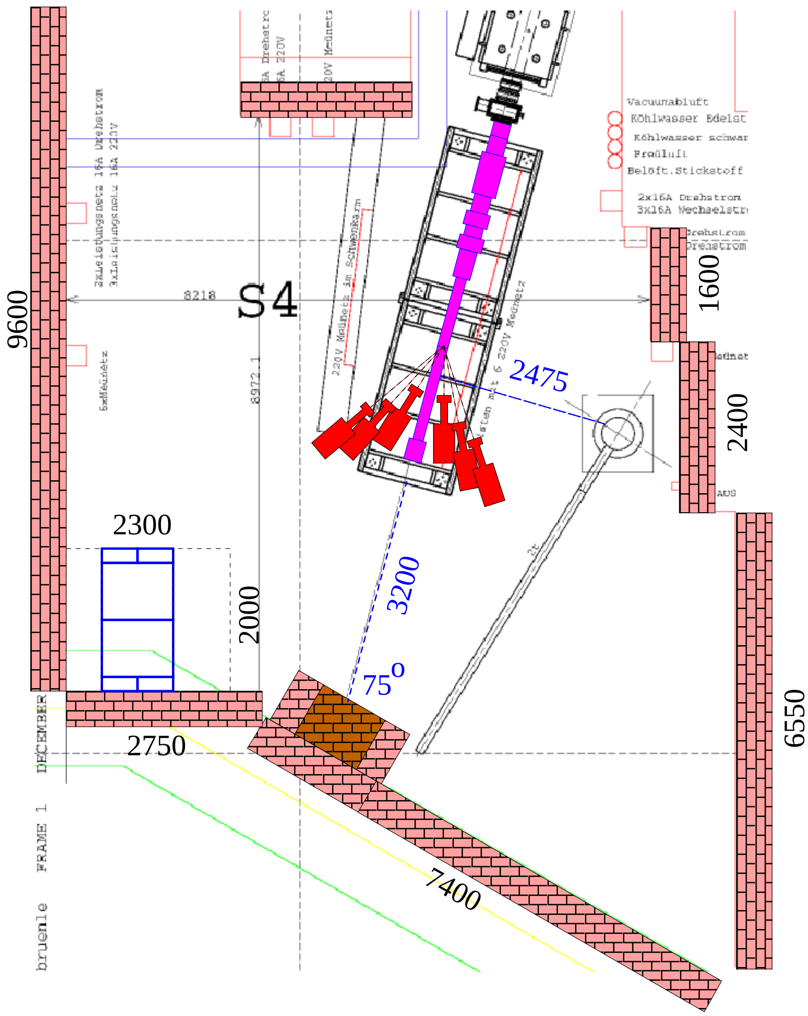

8 Appendix-5:

www.gsi.de/∼wolle/EB_at_GSI/FRS-WORKING/IMAGES/adam.pdf

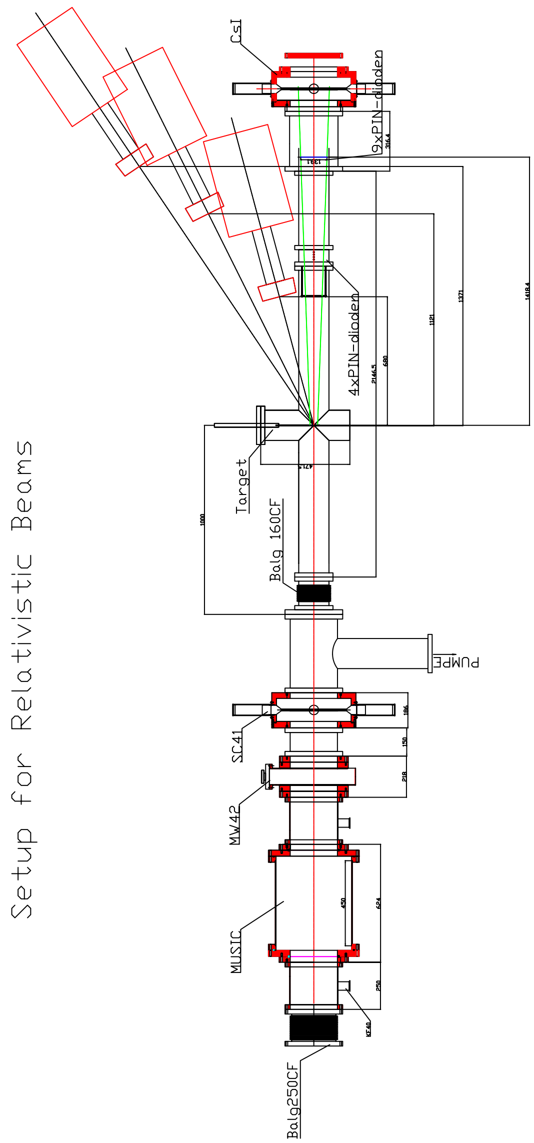

9 Appendix-6:

www.gsi.de/∼wolle/EB_at_GSI/FRS-WORKING/IMAGES/ang_width.gif

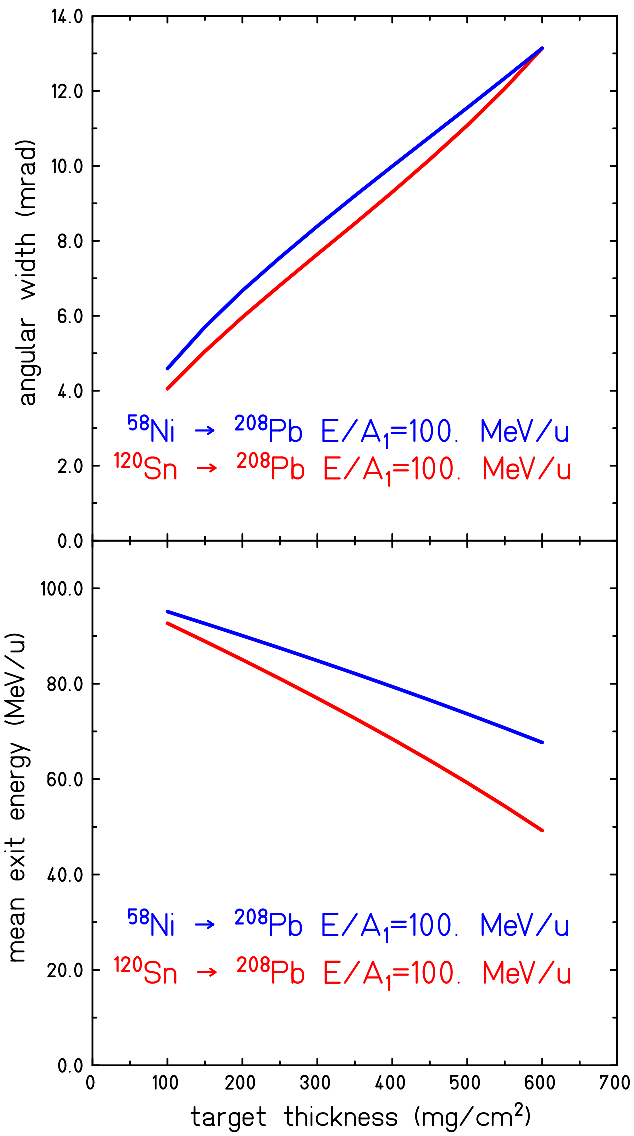

10 Appendix-7:

www.gsi.de/∼wolle/EB_at_GSI/FRS-WORKING/IMAGES/coulex_cross.gif